

AD-A133 321

A LOW LOSS QUASIOPTICAL CAVITY FOR A TWO-STAGE FREE
ELECTRON LASER (FEL)(U) KMS FUSION INC ANN ARBOR MI
S VON LAVEN ET AL. 25 AUG 83 KMSF-U1362

1/1

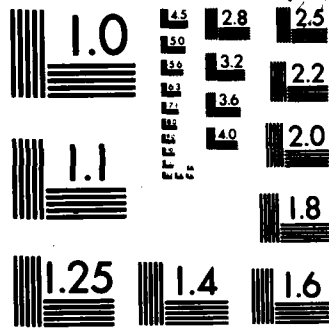
UNCLASSIFIED

N00014-80-C-0614

F/G 20/5

NL





MICROCOPY RESOLUTION TEST CHART
NATIONAL BUREAU OF STANDARDS-1963-A

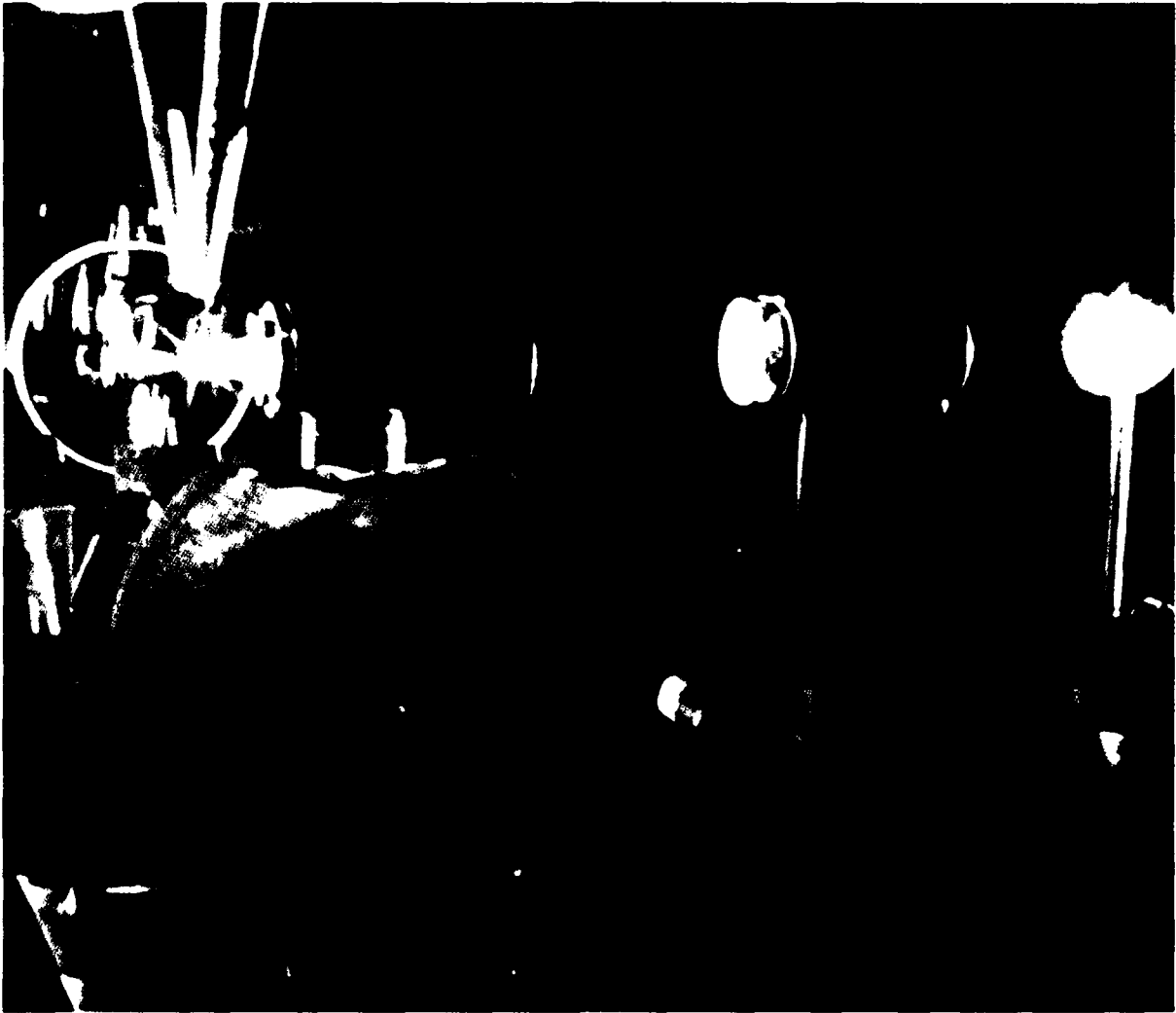
**.kms
fusion**
inc.

A LOW LOSS QUASIOPTICAL CAVITY FOR A TWO-STAGE FEL

S. Von Laven, S. B. Segall and J. F. Ward

DTIC
OCT 7 1983
A

AD-A133 321



DTIC FILE COPY

Submitted to: SPIE (International Society for Optical Engineering)
Bellingham, Washington

This document is approved for public release

REPORT DOCUMENTATION PAGE		READ INSTRUCTIONS BEFORE COMPLETING FORM
1. REPORT NUMBER KMSF-U1362	2. GOVT ACCESSION NO. DAAG23-83-0002	3. RECIPIENT'S CATALOG NUMBER
4. TITLE (and Subtitle) A low loss quasioptical cavity for a two-stage free electron laser (FEL)	5. TYPE OF REPORT & PERIOD COVERED Technical Report	
	6. PERFORMING ORG. REPORT NUMBER	
7. AUTHOR(s) S. Von Laven, S. B. Segall, and J. F. Ward	8. CONTRACT OR GRANT NUMBER(s) N00014-80-C-0614	
9. PERFORMING ORGANIZATION NAME AND ADDRESS KMS Fusion, Inc. 3621 South State Rd., P.O. Box 1567 Ann Arbor, MI 48106	10. PROGRAM ELEMENT, PROJECT, TASK AREA & WORK UNIT NUMBERS	
11. CONTROLLING OFFICE NAME AND ADDRESS Defense Contract Administration Services Management Area, Detroit McNamara Federal Bldg., 477 Michigan Avenue Detroit, MI 48226	12. REPORT DATE August 25, 1983	
	13. NUMBER OF PAGES 11	
14. MONITORING AGENCY NAME & ADDRESS (if different from Controlling Office) Office of Naval Research 1030 Green Street Pasadena, CA 91106	15. SECURITY CLASS. (of this report) Unclassified	
	15a. DECLASSIFICATION/DOWNGRADING SCHEDULE	
16. DISTRIBUTION STATEMENT (of this Report) Unlimited		
17. DISTRIBUTION STATEMENT (of the abstract entered in Block 20, if different from Report)		
18. SUPPLEMENTARY NOTES To be published in the proceedings of the FEL Workshop, held at Eastsound, WA, June, 1983.		
19. KEY WORDS (Continue on reverse side if necessary and identify by block number) Free electron laser, waveguide laser, resonant cavity, two-stage FEL quasioptical cavity, mode conversion, microwave horn <i>approx.</i> <i>free electron laser</i>		
20. ABSTRACT (Continue on reverse side if necessary and identify by block number) A quasioptical cavity consisting of a cylindrical, metallic, overmoded, TE ₀₁ waveguide between two spherical end mirrors will be used to contain long-wavelength (≈ 1 mm) pump radiation in a two-stage FEL. The major loss mechanism is found to be mode conversion. Two different modified cavities are shown to suffer negligible mode conversion, and two more possible approaches, with low mode conversion and additional advantages, are discussed. <i>tbl 1</i>		

II. General features of the TE_{01} cavity

A two-stage FEL cavity must provide interaction regions for both stages, suffer low pump losses, and transmit a fraction of the second-stage radiation. Both the first-stage and second-stage interactions take place in the waveguide where good overlap between the fields and the electron beam can be achieved. The electron beam passes through the second-stage interaction region with the low energy spread necessary for the interaction. Then it passes through the first-stage magnetostatic wiggler, acquiring a relatively large beam energy spread as described elsewhere in this volume.³

The cylindrical waveguide shown in Figure 1 supports the TE_{01} circular mode. The most important field component of this mode is the azimuthal electric field, E_ϕ , which has an annular profile as shown in Figure 2. Beyond the guide this annular mode diverges with a diffraction angle proportional to λ/a , where λ is the pump wavelength and a is the guide radius. The radial profile of E_ϕ remains annular, and the magnitude of E_ϕ near the cavity axis grows smaller. The infrared mode is also annular, but its diffraction angle, proportional to λ_{IR}/a , is much smaller than that of the pump field. Thus annular mirrors permit passage of the infrared mode on axis with low transmission of the 1-mm pump field. As λ/a increases, this mirror-hole loss decreases, but waveguide attenuation increases.

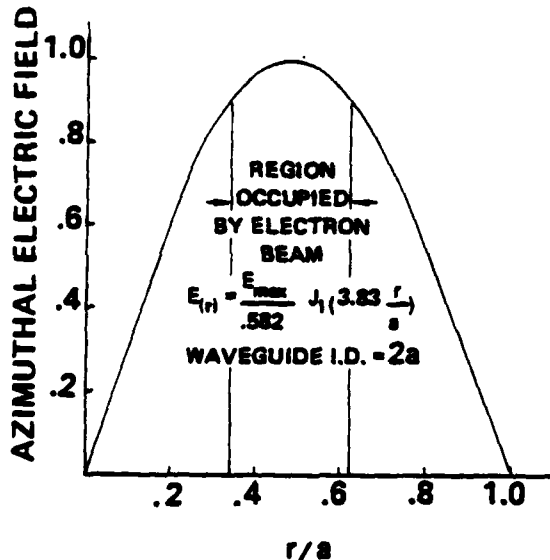


Figure 2. Mirror-hole diffraction losses are low due to annular field distribution.

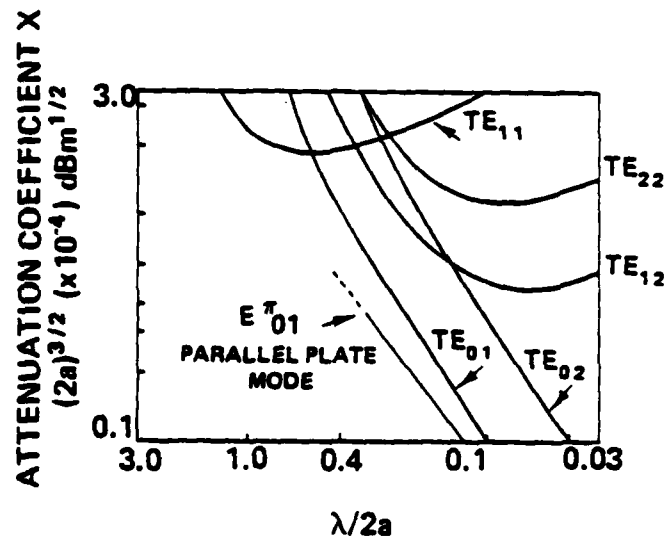


Figure 3. TE_{01} resistive losses are the lowest of any guided mode.

As Figure 3 shows, the TE_{01} mode is the lowest loss mode in an overmoded ($\lambda \ll 2a$) circular waveguide. Conventional rectangular guide has no mode with comparable short-wavelength behavior. Thus the TE_{01} circular mode offers the best combination of guided propagation and low loss. The TE_{02} mode has a factor of four higher attenuation in the waveguide and higher transmission through the mirror holes. Higher-order TE_{0n} modes and all other modes suffer even higher losses.

The wall currents in TE_{01} waveguide are purely azimuthal. Thus, the guide may be segmented axially with little increase in waveguide attenuation. This permits the introduction of an axial electric field for gain optimization. It will also greatly increase the losses for non- TE_{0n} modes.

VII. Mode conversion

Mode conversion, also known as coupling loss, results from the failure of the reflected radiation to duplicate precisely the original TE_{01} mode at the waveguide end. In our analysis, as in previous waveguide laser work,⁴ the radiation propagating between the guide and the mirror is represented as a set of free-space modes, each with a spherical wave front, and the curvature of the spherical mirror is chosen to match these wave fronts. The appropriate modes are the Gauss-LaGuerre $TEM_{p,0}$ modes, for which the azimuthal electric field at the beam waist is given as

$$E_{\phi,p}(u) = \sqrt{\frac{2u}{\pi w_0^2}} L_p^{(1)}(u) \frac{1}{\sqrt{p+1}} e^{-u/2}, \quad (1)$$

where $u = 2r^2/w_0^2$. For convenience, we choose to locate the beam waist at the waveguide end. This condition, together with the matching of wave-front curvature to mirror curvature, determines the beam waist radius w_0 for the complete set of free-space modes. Different values of w_0 are associated with different mirror curvatures.

If the TE_{01} mode at the end of the waveguide is expressed as

$$E'_{\phi} = \sum_{p=0}^{\infty} C_p E_{\phi,p}, \quad (2)$$

then, after the trip to the mirror and back, we have

$$E_{\phi} = \sum_{p=0}^{\infty} C_p E_{\phi,p} \exp(2i\phi_p), \quad (3)$$

where $\phi_p = 2p \tan^{-1}[L\lambda/\pi w_0^2]$, L is the guide-mirror separation, and λ is the pump wavelength. Throughout this paper the mirror diameter is assumed to be large enough to allow us to ignore the radiation lost around the edge. The reconstructed field E'_{ϕ} will not, in general, be equal to E_{ϕ} . This is because the free-space modes suffer a relative phase shift, $2\phi_p$, proportional to their mode number. (See, for example, Kogelnik and Li.⁵) The phase shifts are important because the amplitudes of high-order free-space modes are significant, as seen in Table 1.

When E'_{ϕ} is expanded in terms of TE_{0n} circular-waveguide modes, the fraction of power converted into non- TE_{01} modes is found. This will be small if ϕ_p is close to $p\pi$ or 0. We will be concerned with the former condition, which can also be expressed as

$$L\lambda/\pi w_0^2 \gg 1. \quad (4)$$

Larger guide-mirror separations lead to lower mode conversion. Smaller beam waists (maintaining a fixed ratio of beam waist radius to waveguide radius) also lead to lower mode conversion. Figure 4, which shows the power not in the TE_{01} mode after a single reflection for the case $w_0/a=0.3$, illustrates this behavior clearly. The value $w_0/a=0.3$ is chosen because it minimizes the mode conversion.

These mode conversion values match with results from a Fresnel-Huygens propagation code. The propagation code avoids a free-space mode field representation by calculating the far-field radiation pattern at the mirror directly from the TE_{01} aperture distribution,

Table 1. Free-Space Mode Coefficients.

$w_0/a = 0.300$		$w_0/a = 0.564$		$w_0/a = 0.675$	
Minimum mode conversion loss.		Maximum TE_{01} amplitude.		Peak of TE_{01} mode located at same radius as peak of TE_{01} mode.	
p	C_p	p	C_p	p	C_p
0	0.6153E+00	0	0.9834E+00	0	0.9447E+00
1	-.5828E+00	1	-.6319E-03	1	0.2947E+00
2	0.4400E+00	2	-.1583E+00	2	-.3544E-01
3	-.2695E+00	3	-.4704E-01	3	-.1052E+00
4	0.1139E+00	4	0.3764E-01	4	-.6372E-01
5	-.4748E-02	5	0.4585E-01	5	-.6218E-02
6	-.3733E-01	6	0.1572E-01	6	0.2846E-01
7	0.2040E-01	7	-.1291E-01	7	0.3545E-01
8	0.1125E-01	8	-.2311E-01	8	0.2427E-01
9	-.1388E-01	9	-.1673E-01	9	0.6822E-02
10	-.5760E-02	10	-.3368E-02	10	-.8117E-02
11	0.8875E-02	11	0.8081E-02	11	-.1630E-01

$\sum_{p=0}^{11} C_p^2 = 0.9998$	$\sum_{p=0}^{11} C_p^2 = 0.9992$	$\sum_{p=0}^{11} C_p^2 = 0.9987$
----------------------------------	----------------------------------	----------------------------------

where the aperture is the open waveguide end. F_{ϕ} is then given by the far-field pattern in the plane of the aperture due to the distribution on the mirror.

Guide-mirror separations larger than a few meters are inconvenient experimentally. Reducing the guide radius, a , reduces mode conversion but increases the resistive loss in the waveguide. Electron beam optics also becomes more difficult with a smaller guide diameter. Since we wish to hold the total cavity losses below one percent and maintain a relatively large guide diameter, we would like to reduce mode conversion substantially.

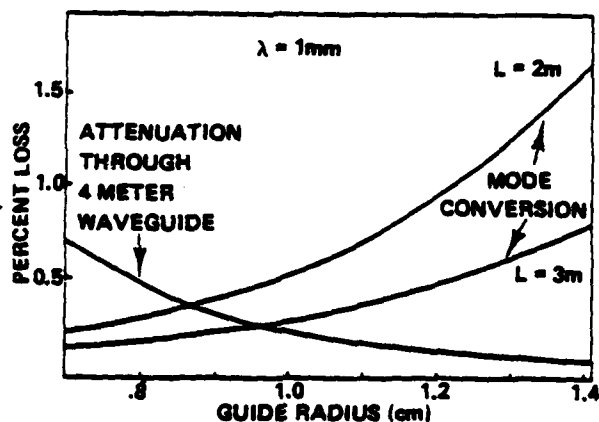


Figure 4. Overmoding trades waveguide attenuation for mode conversion.

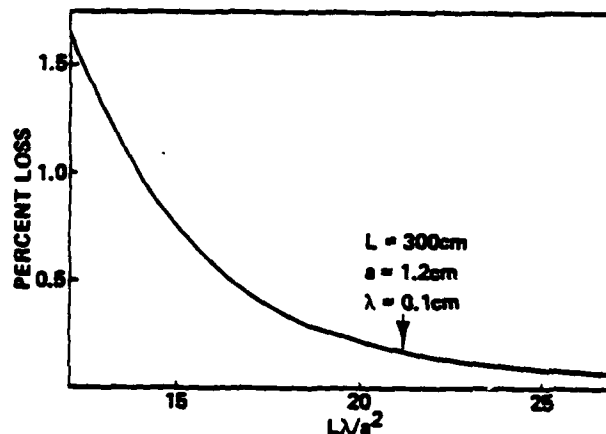


Figure 5. Mirror-hole diffraction is small for likely dimensions.

For example, with $L=3m$ and $a=1.2$ cm, the total round-trip cavity losses are 1.8%. Of this total, 0.9% is due to mode conversion and 0.6% is due to resistive losses in the waveguide and at the end mirrors. Methods of reducing mode conversion to negligible levels are discussed in the next section. To reduce losses further the mirrors and waveguide could be cooled to reduce absorption.

What remains is the diffraction loss through the infrared output coupling hole. This loss depends on the guide radius as well as the guide-mirror separation, L , because for low-loss infrared transmission the hole radius is of the order of the guide radius. Figure 5 shows the dependence of this loss on cavity parameters. In the above example we have $L\lambda/a^2 = 20.8$, which for a symmetric cavity with holes in both mirrors implies a little over 0.3% contribution to the total losses. This loss can be reduced by increasing L .

IV. Improved cavity designs

Four different approaches are described for reducing mode conversion. The first two, involving modified reflectors, have already led to theoretically viable solutions, as will be shown. Work in progress on the horn and closed-cavity approaches is discussed. A less practical fifth approach, phase-conjugate reflection, is also mentioned.

Two-element reflectors

Mode matching with a single spherical reflector, as discussed in Section III, is imperfect unless the guide-mirror separation is ∞ or 0. At intermediate values of the separation, free-space modes with different radial mode numbers arrive back at the waveguide with relative phase shifts as discussed in the previous section, and imperfect reconstruction of the waveguide mode results. A two-element reflector (see Figure 6) provides an additional relative phase shift in the lens-mirror region which can be adjusted to make all round-trip relative phase shifts an integral multiple of 2π . A derivation of the condition which the reflector parameters must satisfy is outlined below.

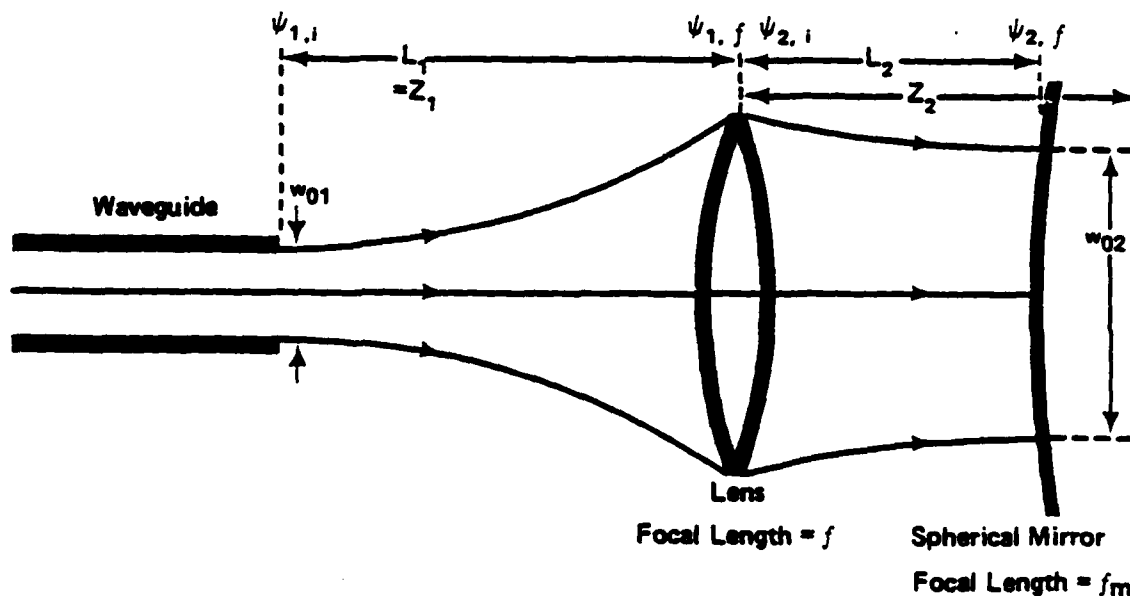


Figure 6. Two-element reflector.

For convenience we define the Rayleigh range, $Z_0 = \pi w_0^2 / \lambda$, where w_0 is again the beam radius at the waist. Let Z_{01} and Z_{02} be the Rayleigh ranges associated with the beam between the waveguide and the lens and the beam between the lens and the mirror, respectively. Distances L_1 , L_2 , focal lengths of lens f and mirror f_m , and lens-beam waist distance Z_2 are shown in Figure 6. The relative phase shifts between successive modes, and associated with the two beams as indicated in Figure 6, are given as follows:

$$\psi_{1,i} = 0 \quad (5a)$$

$$\psi_{1,f} = 2 \tan^{-1}(z_1/z_{01}) \quad (5b)$$

$$\psi_{2,i} = 2 \tan^{-1}(-|z_2|/z_{02}) \quad (5c)$$

$$\psi_{2,f} = 2 \tan^{-1}[-(|z_2| - L_2)/z_{02}]. \quad (5d)$$

The total relative phase shift between successive free-space modes propagating from the waveguide to the mirror is

$$\phi_0 = (\psi_{1,f} - \psi_{1,i}) + (\psi_{2,f} - \psi_{2,i}). \quad (6)$$

Making use of relations between free-space beam parameters (see Reference 5) leads eventually to

$$\phi_0 = 2 \tan^{-1} \left[\frac{fL_1 + fL_2 - L_1L_2}{z_{01}(f - L_2)} \right]. \quad (7)$$

Setting either the numerator or denominator equal to zero in the argument appearing in Equation 7 gives the result that ϕ_0 is some multiple of π . Thus, the round trip relative phase shift for all free-space modes is an integral multiple of 2π .

We examine the latter case, $f=L_2$, and make the further simplification $L_1=L_2=f$. In this case we also find $z_{01}z_{02}=f^2$ and $z_2=L_2$. The result for z_2 implies that the mirror is located at the second beam waist and, thus, will be flat ($f_m=\infty$). With L_1 equal to L_2 , we can easily fold the optical system by replacing the lens with a reflector of focal length f and moving the flat to the end of the waveguide. Figure 7 indicates the ray paths in such a system and lists parameters associated with a 3m separation. Radiation reentering the waveguide directly from the curved mirror without reflecting off the plane mirror is not correctly conditioned for mode matching. However, the field is small near the axis for the TEM_{00} modes so that this mismatch is insignificant for a 3m separation.

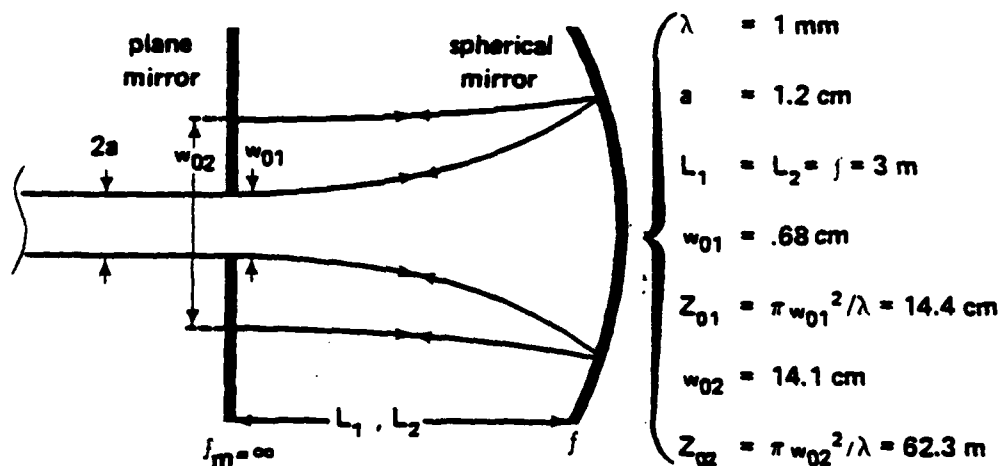


Figure 7. Folded two-element reflector with 3m separation.

Thus, without increasing the overall cavity length, mode conversion losses can be made negligible. In the 3m case this eliminates a 0.9% loss, while introducing a separation-independent 0.6% absorption loss due to the four additional reflections. Cooling would now be even more desirable. Total round-trip losses could be reduced from 1.5% to about 0.9% with liquid nitrogen or to about 0.3% with liquid helium.

Wave-front reflector

Another approach to the reduction of mode conversion requires figuring of the mirror surface to match the incident wave front of the total field, given by the sum of the free-space modes. Such a mirror simultaneously reverses the propagation direction of the entire wave front, which then follows exactly in reverse the evolution undergone during propagation from the waveguide to the mirror. No phase conjugation occurs; only carefully controlled conventional reflection is required. In terms of free-space modes, one can say that the mirror reduces the optical path length for each higher-order mode by the amount required to compensate for the relative phase shifts by making use of each mode's unique transverse profile. Thus, the phase shifts vanish, and the returning radiation precisely duplicates the original TE_{01} mode.

The total electric field along a surface of uniform phase can be written

$$E_{\phi} = \left[\sum_{p=0}^{\infty} C_p \frac{w_0}{w} L_p^{(1)}(u) e^{-u/2} \exp[-i(kz - \phi_p) - r^2(1/w^2 + ik/2R)] \right] e^{i\omega t}, \quad (8)$$

where

$$\text{Im} \left[\sum_{p=0}^{\infty} C_p L_p^{(1)}(u) \exp(i\phi_p) \right] = 0 \quad (9)$$

with $\phi_p = 2p \tan^{-1}(z/z_0)$ and $u = 2r^2/w^2$. The coefficients C_p include the normalization constants. Here, R is the radius of curvature of the wave fronts of the individual modes, and w is the beam radius at arbitrary z . R and w are given as

$$R = z(1 + z_0^2/z^2) \quad (10a)$$

$$w^2 = w_0^2 (1 + z_0^2/z^2). \quad (10b)$$

The condition imposed by Equation 9 determines $z(r)$ for an arbitrarily selected value of the overall phase at a fixed time. No generality is lost in making this selection. Equation 9 can be solved numerically for z .

In order to be sure of achieving low mode conversion, we will need to evaluate the errors introduced by the paraxial approximation in each of the prospective cavity designs. For example, spherical mirrors might be replaced by parabolic mirrors. If non-paraxial corrections to the mirror figure are required, they could most easily be implemented as a modification to the wave-front reflector, since aspherizing is already necessary. No additional absorption losses would be incurred as with the two-element reflector.

Horns

An appealing solution to the mode conversion problem would be to convert the TE_{01} waveguide mode to the lowest order free-space mode with very little power in higher-order free-space modes. Relative phase shifts between modes would then have no significance. This approach would require specially designed horns on the ends of the waveguide. In addition to reducing mode conversion, such horns would radiate a cleaner far-field pattern than the open pipe, permitting a larger mirror-hole diameter and a smaller overall mirror diameter. Horns may also be the least expensive solution to implement.

Horns are commonly designed with the goal of reducing the side lobes present in the radiation patterns of open-ended, single-mode waveguides. Side lobes imply the presence of high-order free-space modes. Thus our design criteria will be similar to those commonly used, but they will be more stringent.

The closest approach to the required horn design seems to be the aperture-matched horn reported by Burnside and Chuang.⁶ Flared surfaces attached to the end of a conventional horn have been found theoretically and experimentally to reduce side lobe power levels by roughly a factor of three below the already low levels present in the pattern produced by the unmodified horn (see Figure 8). The unmodified horn is similar to our open-ended waveguide in that a single mode is incident upon an aperture which has dimensions large compared to a wavelength. Thus, a flared surface may be able to reduce mode conversion.

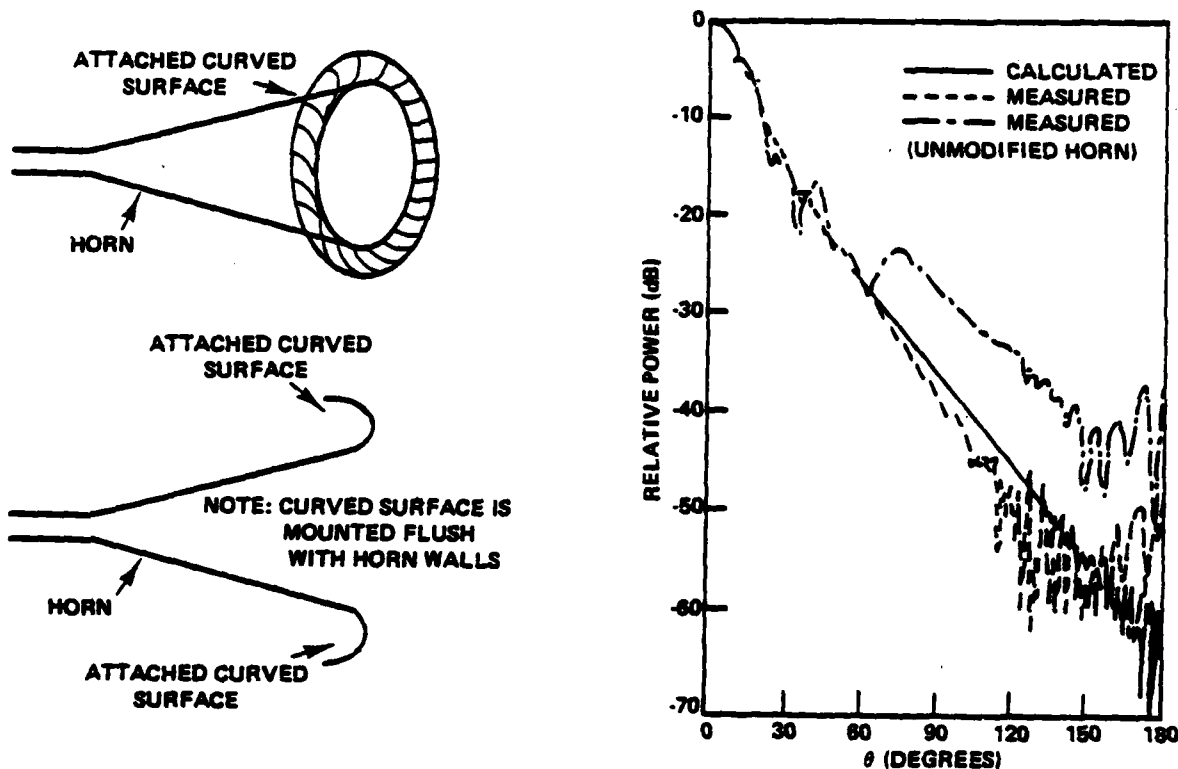


Figure 8. (a) Aperture-matched horn (after Ref. 6, copyright 1982 IEEE).

(b) F-plane pattern of aperture-matched rectangular horn (after Ref. 6, copyright 1982 IEEE).

The contours discussed in Reference 6 are probably not adequate for the performance we require. Ideally, a design procedure should be created in which an optimum or near-optimum contour is found as a function of the coupling between the TE_{01} waveguide mode and the TE_{01} free-space mode. Such a design procedure exists for the simpler problem of a nonlinear taper, which couples the TE_{01} mode in circular waveguide to the same mode in a waveguide of different diameter by carefully controlling the TE_{02} power in the taper.⁷ Adaptation of this procedure to our problem must account for many unwanted modes rather than only one.

Closed cavity

A different approach is to enclose completely the region between the waveguide and the spherical mirror with a tapered waveguide as shown in Figure 9. If the maximum taper

angle, θ_0 , is no more than a few degrees, then only the lowest two cone modes are required to represent the field in the tapered region adequately.

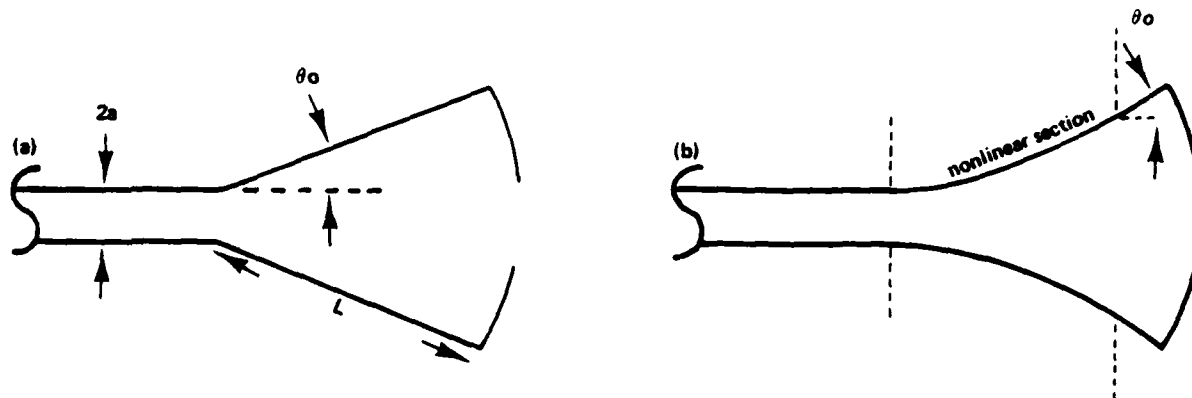


Figure 9. (a) Closed cavity with a linear taper.

(b) Closed cavity with a nonlinearly tapered section.

The TE_{0n} cone modes are given by

$$E_{\phi,n}(\theta,R) = \frac{C}{\sqrt{P}} R_{\nu_n+1/2}^{(2)}(kR) \frac{d}{d\theta} [P_{\nu_n}(\cos\theta)], \quad (11)$$

where n is the transverse mode number. Azimuthal symmetry is assumed. C is a constant, R is the distance from the cone's vertex, k is the free-space wavenumber and θ is the angle with respect to the cone's axis. $R^{(2)}$ and P are, respectively, the Hankel function of the second kind and the associated Legendre function. The order of each function is indicated by a subscript, which is positive but not, in general, an integer. The ν_n ($n=1,2,3 \dots$) are a discrete set of numbers which are found numerically by satisfying the condition

$$E_{\phi,n}(\theta_0,R) = 0. \quad (12)$$

The TE_{0n} cone modes are very similar to the TE_{0n} circular-waveguide modes. Thus, the best cavity performance would be obtained by arranging for only the TE_{01} mode to be incident upon the mirror. As in the case of the lowest-order free-space mode, this permits a large mirror-hole diameter and relatively smaller overall mirror diameter. Good conversion to the TE_{01} cone mode could be achieved by the nonlinear section of the compound taper shown in Figure 9b. This could be designed according to the procedure given in Reference 7 with little modification.

The simpler case of a linear taper (Figure 9a) is examined briefly here. About one percent of the power is allowed to propagate in the TE_{02} cone mode and smaller fractions in higher-order modes. These fractions are found by expanding the incident TE_{01} circular-waveguide mode in terms of the functions given in Equation 11, accounting for the phase variation of the incident mode along a constant-phase spherical surface of the cone modes. As in the free-space case, E_{ϕ}' is evaluated including the relative phase shifts accumulated by the cone modes propagating to the mirror and back. The phase shifts are found by evaluating the Hankel function in Equation 11. Then E_{ϕ}' , in turn, is expanded in terms of TE_{0n} circular-waveguide modes in order to determine the mode conversion.

Some results are displayed in Figure 10. The minima occur when the length of the taper is sufficient to introduce approximately 180° of relative phase shift between the first two cone modes. Arriving back at the waveguide, the TE_{01} cone mode converts into a TE_{01} circular mode and a smaller amplitude TE_{02} mode. The TE_{02} cone mode converts mostly to the TE_{02} circular mode. When the phase shift is 180° , these two TE_{02} waves approximately cancel, nearly eliminating the major contribution to mode conversion in the closed cavity. The relative phase shifts are smaller as the diameter increases. Thus, a greater length is required to accumulate the necessary 180° as Figure 10 shows.

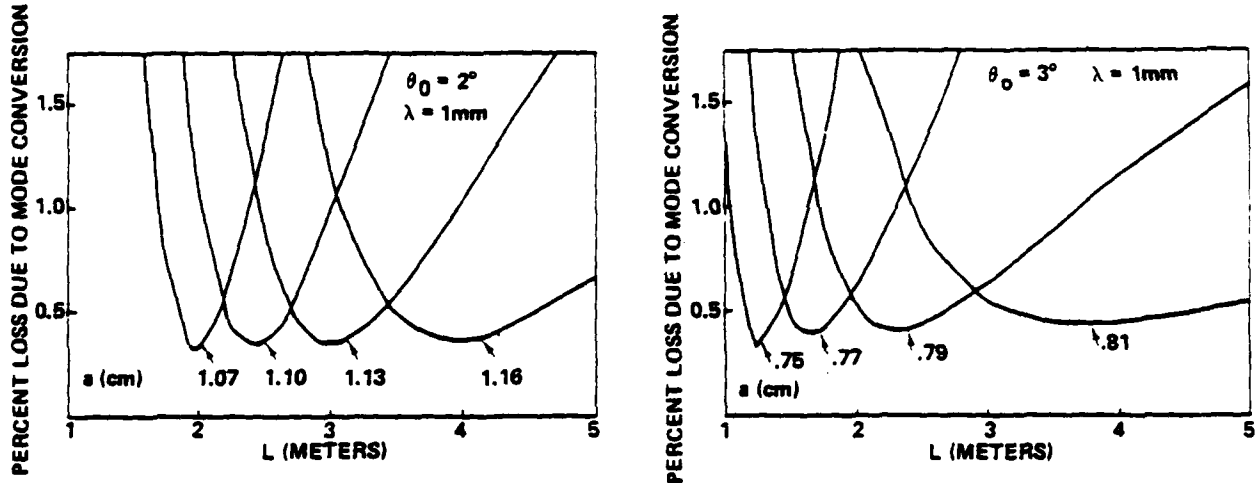


Figure 10. (a) Closed-cavity mode conversion vs. linear taper length with $\theta_0 = 2^\circ$.

(b) $\theta_0 = 3^\circ$.

The choice of taper angle involves a tradeoff between mode conversion and a reasonable taper length to reach the diameter required to couple out the infrared radiation. The power in higher-order cone modes increases quickly above $\theta = 3^\circ$. The waveguide diameter can then be chosen to minimize the loss through the mirror hole (which again has roughly the same diameter as the waveguide) and the loss due to waveguide attenuation. Figure 11 shows the tradeoff associated with this choice.

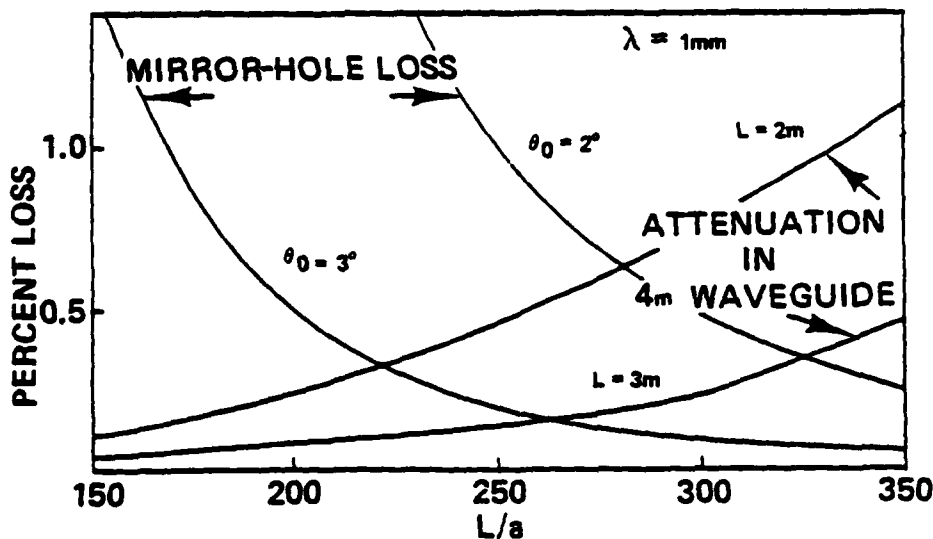


Figure 11. In the closed cavity a tradeoff exists between mirror-hole loss and waveguide attenuation.

Phase-conjugate reflectors

Phase-conjugate reflectors have been considered for use as end mirrors.⁸ There would be no mode conversion with such reflectors. However, the efficiency of present phase conjugators is low by our standards, either through low reflectivity or large power requirements. Higher efficiency may result as researchers continue their efforts.

V. Conclusions

Mode conversion is identified as a major loss mechanism in a TE_{01} quasioptical cavity. Two possible cavity modifications are shown to eliminate mode conversion. These are the two-element reflector and the wave-front reflector. Two other approaches, the horn and the closed cavity may be able to reduce both mode conversion and mirror hole losses. The use of phase-conjugate reflectors depends on future demonstration of efficient operation.

IV. Acknowledgements

We wish to thank Dr. George Busch of KMS Fusion and Dr. Barry Feldman of the Air Force Office of Scientific Research for helpful suggestions. This work is supported by the Office of Naval Research under Contract No. N00014-80-C-0614.

VII. References

1. Elias, L. R., "High Power, cw, Efficient, Tunable (UV through IR) Free-Electron Laser Using Low-Energy Electron Beams," Phys. Rev. Lett., Vol. 42, pp. 977-981 (1979).
2. Secall, S. R., Takeda, H., Von Laven, S., Diamant, P., and Ward, J. F., "The KMS Fusion, Inc. Two-Stage Free Electron Laser Program," in this volume.
3. Takeda, H. and Secall, S. R., "Limiting Energy Spread at High Laser Intensities Using Phase Space Displacement," in this volume.
4. Deenan, J. J., "The Waveguide Laser: A Review," Appl. Phys., Vol. 11, pp. 1-33 (1976).
5. Kogelnik, H. and Li, T., "Laser Beams and Resonators," Appl. Opt., Vol. 5, pp. 1550-1567 (1966).
6. Burnside, W. D. and Chuang, C. W., "An Aperture-Matched Horn Design," IEEE Trans. on Antennas and Propagation, Vol. AP-30, pp. 790-796 (1982).
7. Hecken, R. P. and Anuff, A., "On the Optimum Design of Tapered Waveguide Transitions," IEEE Trans. on Microwave Theory and Techniques, Vol. MTT-21, pp. 374-380 (1973).
8. Roulnois, J. L., Agrawal, G. P., "Waveguide Resonators with Mode Discrimination and Coupling Losses in Rectangular-Conventional and Phase-Conjugate Mirrors," J. Opt. Soc. Am., Vol. 72, pp. 853-860 (1982).

I. Distribution List

Director
Defense Advanced Research Projects
Agency
(3 copies)
Attn: Technical Library
1400 Wilson Boulevard
Arlington, VA 22209

Office of Naval Research
(3 copies)
Physics Division Office (Code 412)
800 North Quincy Street
Arlington, VA 22217

Office of Naval Research
Director, Technology (Code 200)
800 North Quincy Street
Arlington, VA 22217

Naval Research Laboratory
(3 copies)
Department of Navy
Attn: Technical Library
Washington, DC 20375

Office of the Director of Defense
Research and Engineering
(3 copies)
Information Office Library Branch
The Pentagon
Washington, DC 20301

U.S. Army Research Office
(2 copies)
Box 1211
Research Triangle Park, NC 27709

Defense Technical Information Center
(12 copies)
Cameron Station
Alexandria, VA 22314

Director, National Bureau of Standards
Attn: Technical Library
Washington, DC 20234

Commanding Officer
(3 copies)
Office of Naval Research Western
Detachment Office
1030 East Green Street
Pasadena, CA 91101

Commanding Officer
(3 copies)
Office of Naval Research
Eastern/Central Detachment Office
495 Summer Street
Boston, MA 02210

Commandant of the Marine Corps
Scientific Advisor (Code RD-1)
Washington, DC 20380

Naval Ordnance Station
Technical Library
Indian Head, MD 20640

Naval Postgraduate School
Technical Library (Code 5632.2)
Point Mugu, CA 93010

Naval Ordnance Station
Technical Library
Louisville, KY 40214

Commanding Officer
Naval Ocean Research & Development
Activity
Technical Library
NSTL Station, MS 39529

Naval Explosive Ordnance Disposal
Facility
Technical Library
Indian Head, MD 20640

Naval Ocean Systems Center
Technical Library
San Diego, CA 92152

Naval Surface Weapons Center
Technical Library
Silver Springs, MD 20910

Naval Ship Research & Development
Center
Central Library (Code L42 and L43)
Bethesda, MD 20084

Naval Avionics Facility
Technical Library
Indianapolis, IN 46218

END

FILMED

10-83

DTIC